Dissecting indirect genetic effects from peers in laboratory mice

Amelie Baud[1,2*], Francesco Paolo Casale[1,3], Amanda M. Barkley-Levenson[2], Nilgoun Farhadi[2], Charlotte Montillot[4], Binnaz Yalcin[4], Jerome Nicod[5], Abraham A. Palmer[2,6], Oliver Stegle[1,7*]

[1] European Molecular Biology Laboratory, European Bioinformatics Institute, Wellcome Genome Campus, CB10 1SD Hinxton, Cambridge, UK

[2] Department of Psychiatry, University of California San Diego, La Jolla, CA, 92093, USA

[3] Microsoft Research New England, Cambridge, Massachusetts, USA

[4] INSERM U1231 GAD Laboratory, 21070 Dijon, France

[5] The Francis Crick Institute, London NW1 1AT, UK

[6] Institute for Genomic Medicine, University of California San Diego, La Jolla, CA, 92093, USA

[7] European Molecular Biology Laboratory, Genome Biology Unit, Heidelberg, DE

* Corresponding authors: abaud@ebi.ac.uk and oliver.stegle@embl.de

Abstract

The phenotype of one individual can be affected not only by the individual's own genotypes (direct genetic effects, DGE) but also by genotypes of interacting partners (indirect genetic effects, IGE). IGE have been detected using polygenic models in multiple species, including laboratory mice and humans. However, the underlying mechanisms remain largely unknown. Genome-wide association studies of IGE (igeGWAS) can point to IGE genes, but have not yet been applied to non-familial IGE arising from "peers" and affecting biomedical phenotypes. In addition, the extent to which igeGWAS will identify loci not identified by dgeGWAS remains an open question. Finally, findings from igeGWAS have not been confirmed by experimental manipulation.

We leveraged a dataset of 170 behavioural, physiological and morphological phenotypes measured in 1,812 genetically heterogeneous laboratory mice to study IGE arising between same-sex, adult, unrelated laboratory mice housed in the same cage. We developed methods for igeGWAS in this context and identified 24 significant IGE loci for 17 phenotypes (FDR < 10%). There was no overlap between IGE loci and DGE loci for the same phenotype, which was consistent with the moderate genetic correlations between DGE and IGE for the same phenotype estimated using polygenic models. Finally, we fine-mapped seven significant IGE loci to individual genes and confirmed, in an experiment with a knockout model, that *Epha4* gives rise to IGE on stress-coping strategy and wound healing.

Our results demonstrate the potential for igeGWAS to identify IGE genes and shed some light into the mechanisms of peer influence.

Keywords

Indirect genetic effects; Social genetic effects; Peer effects; Complex traits; Genotype to phenotype; Genome-wide association study

Background

The phenotype of an individual can be affected not only by the individual's own genotypes (direct genetic effects, DGE) but also by environmental factors, including the genotypes of other, interacting individuals (indirect genetic effects, IGE)(1-3) (**Figure 1a**). IGE arise when the phenotype of a focal individual is influenced by heritable traits of interacting partners (**Figure 1b**), which can include behavioural and non-behavioural traits of partners as well as modifications of the non-social environment by partners(4). IGE have been detected in many laboratory systems(5-14), livestock(15-17), crops(18), wild animals(19-21), and humans(22-27), demonstrating that they are an important component of the genotype to phenotype path and an aspect of the environment that can be studied using genetic approaches.

Most prior studies of IGE have used polygenic modelling approaches to study aggregate genetic effects, either studying IGE mediated by *specific traits of partners* using trait-based models(2, 28) or polygenic risk scores(22, 25), or detecting IGE mediated by *unknown heritable traits of partners* using variance components models(9, 15, 29, 30). More recently, the genome-wide association study of IGE (igeGWAS) has been proposed as a strategy to identify individual genetic loci underlying IGE associations(5, 7, 8, 11, 31-35).

However, igeGWAS has only been applied in limited settings: in particular, it has not been used to study non-familial IGE from peers affecting biomedical

phenotypes, despite growing evidence from polygenic models in laboratory mice(9) and in humans(25) that such effects are important. Moreover, the relationship between DGE and IGE affecting the same phenotype has not been fully addressed, such that the scope for igeGWAS to identify loci not detected by dgeGWAS is unknown. Finally, the results of igeGWAS have not yet been translated into experimentally validated genes causing IGE.

To address these issues, we leveraged a published dataset of 170 behavioural, physiological and morphological phenotypes measured in 1,812 male and female, genetically heterogeneous mice (**Figure 1c**), which we supplemented with previously unreported cage information (**Supplementary Table 1**). For each phenotype we investigated the relationship between DGE and IGE, using both polygenic analyses and GWAS. For 17 phenotypes, we fine-mapped IGE loci to identify putative causal genes underlying IGE. Finally, we validated one such gene using a knockout model.

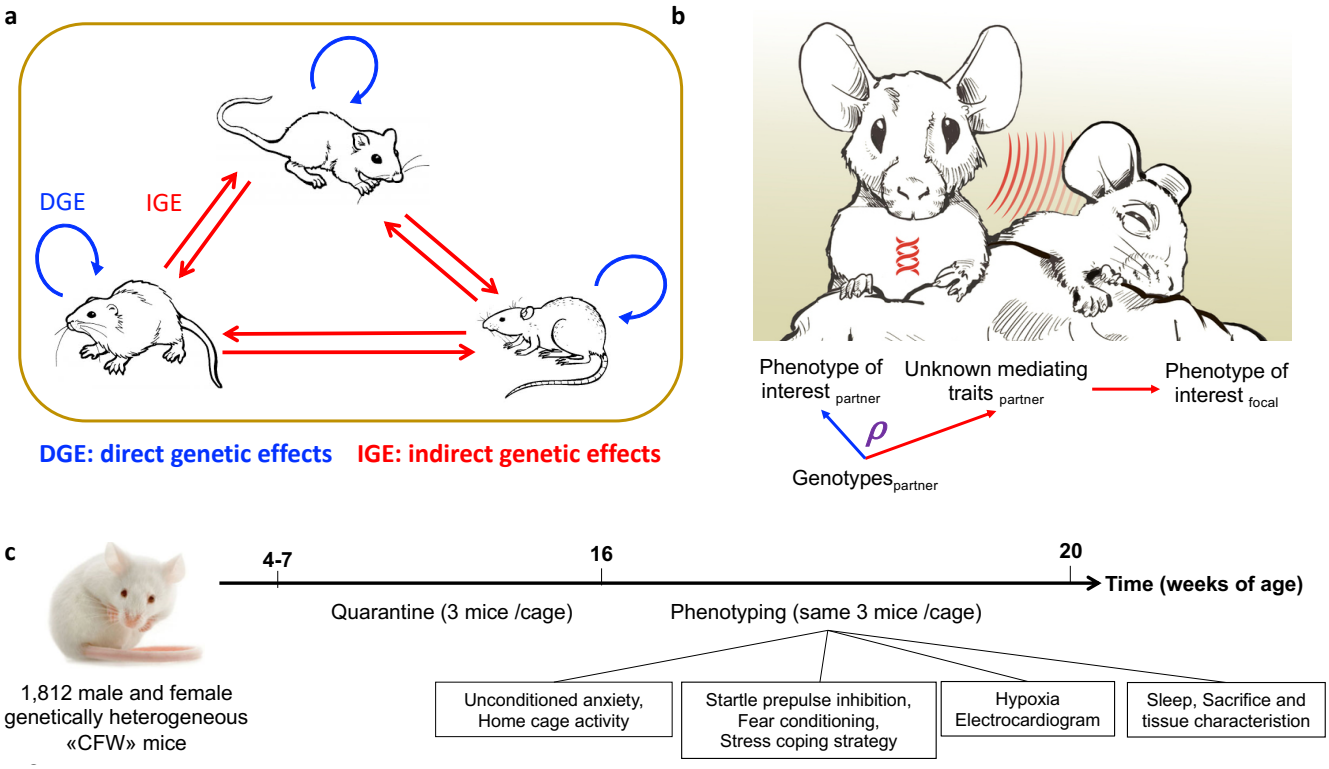

83 ***Figure 1*** *Definition of direct and indirect genetic effects and experimental design.* ***(a)***
84 *Direct genetic effects (DGE, blue) on an individual's phenotype arise from the*
85 *individual's own genotypes; indirect genetic effects (IGE, red) arise from genotypes of*
86 *interacting partners (cage mates). This panel illustrates a situation where all*
87 *individuals are genetically heterogeneous and both DGE and IGE arise from each*
88 *individual's genotypes.* ***(b)*** *IGE on a phenotype of interest arise when two individuals*
89 *interact and (unknown) heritable traits of one individual, the social partner, influence*
90 *the phenotype of interest measured in the other individual. For a given phenotype of*
91 *interest, the correlation* ρ *between DGE and IGE is equivalent to the correlation*
92 *between DGE on the phenotype of interest and DGE on the traits mediating IGE on*
93 *the phenotype of interest. Importantly, this correlation can be estimated even when*
94 *the traits mediating IGE are not known or not measured.* ***(c)*** *Experimental design. A*
95 *list of the 170 phenotypes collected on each mouse is presented in Supplementary*
96 *Table 2.*
97

98 # Results

99 We used the genome-wide genotypes (both LD-pruned and unpruned genotypes
100 derived from low-coverage (0.15×), Illumina sequencing, see Methods) and 200
101 phenotypes for 2,073 commercially available, outbred Crl:CFW(SW)-US_P08(36)
102 (herafter CFW) mice reported in Nicod et al. (37) and Davies et al. (38). In addition,
103 we used previously unreported cage information provided by the authors of the original
104 study upon request (**Supplementary Table 1**). Mice were housed in same-sex groups
105 of three and interacted for at least nine weeks before phenotyping. We excluded any
106 animal whose cage mates changed over the course of the experiment, as well as

107 suspected siblings to rule out confounding from parental and litter effects. These steps
108 resulted in a final sample size of 1,812 mice (927 females, 885 males) for analysis.
109 We normalised each phenotype and excluded 30 phenotypes that could not be
110 satisfactorily normalised (see Methods), yielding a total of 170 phenotypes measured
111 in between 844 and 1,729 mice.

112 **Polygenic analysis of the correlation between DGE and IGE**

113 Initially, we used polygenic models to assess the extent to which loci are shared
114 between DGE and IGE affecting the same phenotype. Briefly, for each trait, we
115 estimated the genetic correlation ρ between DGE and IGE. As this correlation is
116 equivalent to the correlation between DGE on the phenotype of interest and DGE on
117 the traits of partners mediating IGE (**Figure 1b**), a correlation coefficient of 0 would
118 indicate that the traits mediating IGE are genetically uncorrelated (in the classical
119 sense) to the phenotype of interest, whereas a correlation coefficient of ±1 would
120 indicate that the phenotype of interest itself mediates IGE. For 28 traits with evidence
121 for marginal DGE and IGE (>5% variance explained; **Supplementary Figure 1**), we
122 performed hypothesis tests for both models (**Figure 2** and **Supplementary Table 2**).
123 We found that ρ was different from zero for ten out of twenty eight phenotypes ($P <$
124 0.05), indicating that, often, the traits mediating IGE on a phenotype of interest are
125 genetically correlated (in the classical sense) with the phenotype of interest. Evidence
126 that ρ was different from zero was strongest for mean weight of the adrenal glands,
127 which correlates with stress(39), mean platelet volume, LDL cholesterol levels, and
128 rate of healing from an ear punch. Second, ρ was different from plus or minus one for
129 ten phenotypes ($P < 0.05$), with the strongest evidence for a measure of stress-coping
130 strategy (immobility in the forced swim test) and rate of healing from an ear punch.
131 These results indicate that IGE on a phenotype of interest are often mediated by traits

of partners other than the phenotype of interest. To uncover those traits, we turned to igeGWAS.

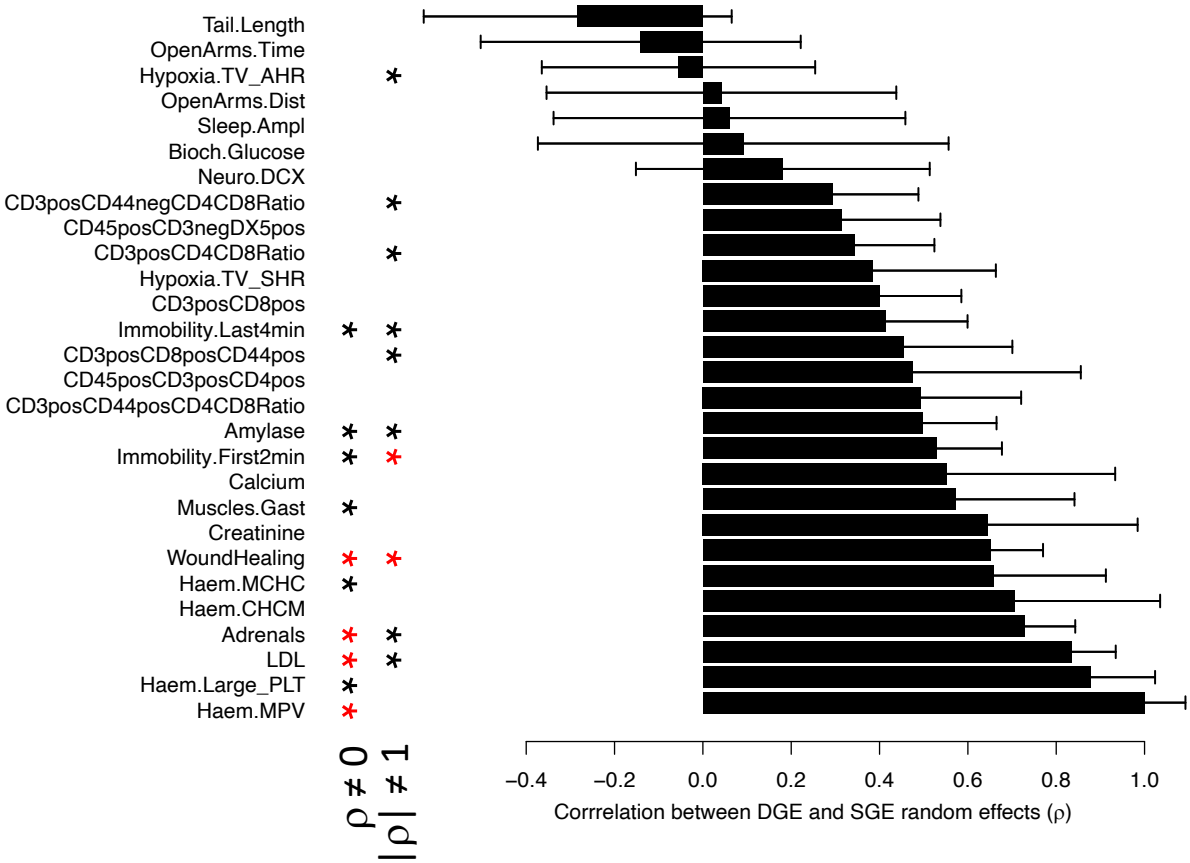

Figure 2 *Correlation coefficients ρ between DGE and IGE estimated using polygenic models. ρ is shown for 28 phenotypes with marginal DGE and IGE greater than 5%. Error bars denote standard errors. Asterisks on the left show phenotypes for which ρ is significantly different from 0 (black: P < 0.05, red: Bonferroni-corrected P < 0.05). Asterisks on the right show phenotypes for which |ρ| is significantly different from 1 (black: P < 0.05, red: Bonferroni-corrected P < 0.05). Numerical values are provided in Supplementary Table 2.*

igeGWAS and dgeGWAS of 170 phenotypes

145 Next, to compare DGE and IGE at the level of individual loci, we considered the LD-
146 pruned set of variants and performed igeGWAS and dgeGWAS in an analogous
147 manner for each one of the 170 phenotypes. For igeGWAS, we estimated the "social
148 genotype" of a mouse at a variant as the sum of the reference allele dosages across
149 its two cage mates at the variant(31, 40), and tested for association between this social
150 genotype and the phenotype of interest. To avoid spurious associations, we accounted
151 for background IGE, background DGE and shared environmental (cage) effects using
152 random effect components in a linear mixed model (Methods). Additionally, we
153 included a fixed effect covariate for DGE arising from the tested variant in igeGWAS.
154 This approach accounts for correlations between direct and social genotypes that
155 arise when each individual serves as both focal individual and social partner in the
156 analysis, a strategy that maximises sample size when all the individuals are genotyped
157 and phenotyped(31, 40). Accounting for such correlations was required to obtain
158 appropriately calibrated P values in our cohort (**Supplementary Figure 2**), and
159 theoretical considerations show that it is required even when considering strictly
160 unrelated samples (**Supplementary Note**). Finally, we adapted previous
161 strategies(37, 41, 42) based on genome-wide permutations to control the per-
162 phenotype FDR (see Methods), thereby accounting for the specific patterns of linkage
163 disequilibrium present in the sample.

164 igeGWAS identified a total of 24 significant loci across 17 of the 170 tested
165 phenotypes (FDR < 10%), including measures relevant to behavior, adult
166 neurogenesis, blood biochemistry, red and white blood cells, apparent bone mineral
167 content, electrocardiography, and ventilatory responses to acute hypoxia
168 (**Supplementary Table 3**). The 17 phenotypes with one or more IGE loci tended to
169 have a higher aggregate contribution of IGE (across the genome) than phenotypes

170 without significant IGE loci (averages of 3.8% and 2.8% respectively), a trend that was
171 not significant (one-sided t-test P = 0.14).

172 To enable a direct comparison between igeGWAS and dgeGWAS, we
173 performed dgeGWAS for each phenotype using the same approach as taken for
174 igeGWAS, including random effects for DGE and IGE polygenic effects and cage
175 effects and including a fixed effect covariate for IGE arising from the tested variant.
176 This identified 120 significant DGE loci for 63 phenotypes (FDR<10%;
177 **Supplementary Table 4**). Consistent with the difference in the number of discoveries,
178 we observed that significant IGE loci had, on average, lower effect sizes (proportion
179 of phenotypic variance explained) than DGE loci (**Supplementary Figure 3**). In light
180 of the observed effect sizes and due to the winner's curse (or Beavis effect (43, 44)),
181 we expect a larger proportion of significant IGE loci to be false associations, compared
182 to significant DGE loci.

183 There was no overlap between significant DGE and IGE loci for the same
184 phenotype, or even for related phenotypes (**Figure 3**). This observation was expected
185 based on the moderate values observed for the correlation ρ between DGE and IGE
186 and the limited power of dgeGWAS and igeGWAS. However, we identified further
187 reason why dgeGWAS and igeGWAS might identify different loci: using simulations to
188 identify key parameters determining the power of igeGWAS, we found that both the
189 number of cage mates and the mode of aggregation across cage mates (i.e. whether
190 the IGE received by a focal mouse correspond to the sum or the average of the IGE
191 emitted by its cage mates) are important, in addition to the parameters also
192 determining the power of dgeGWAS, namely minor allele frequency (MAF) and allelic
193 effect (**Supplementary Figure 4**). Thus, for a given MAF, allelic effect, and a number
194 of cage mates equal to two as is the case in this study, dgeGWAS is expected to have

195 greater power than igeGWAS if IGE get averaged across the two cage mates, but
196 igeGWAS is expected to have greater power than dgeGWAS if IGE sum up across
197 the two cage mates. As sample sizes increase for dgeGWAS and igeGWAS, the
198 moderate genetic correlation ρ between DGE and IGE and the differences in power
199 between dgeGWAS and igeGWAS dictated by the number of cage mates and the
200 mode of aggregation across cage mates (sum or average) will continue to drive the
201 identification of different loci by dgeGWAS and igeGWAS.

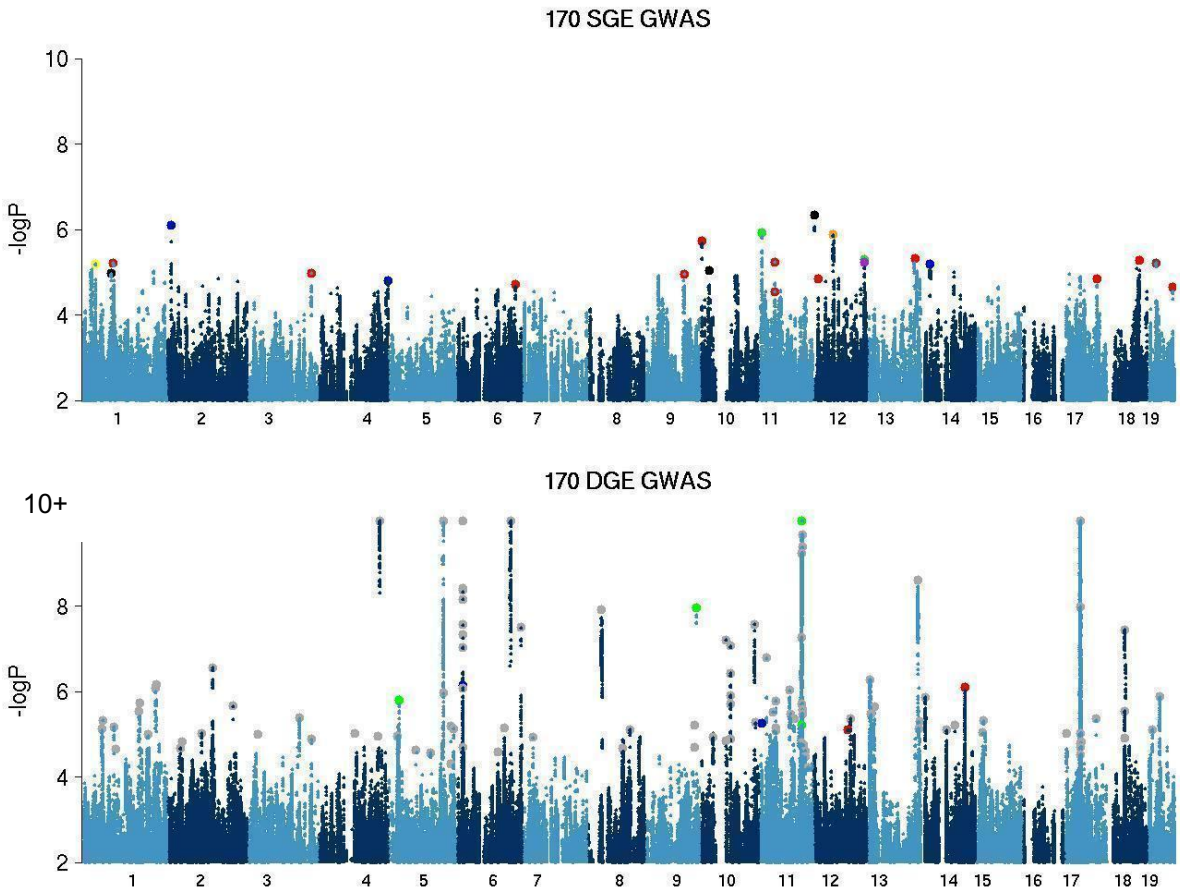

202

203 ***Figure 3*** *Superimposed Manhattan plots corresponding to igeGWAS (top panel) and*
204 *dgeGWAS (bottom panel) of the same 170 phenotypes. DGE associations with a*
205 *negative log P value greater than 10 were truncated at this threshold (as indicated by*
206 *10+); also, data points with negative log P values smaller than 2 are not shown. The*
207 *larger dots correspond to the most significant variant at each significant IGE or DGE*

208 *locus (FDR < 10%). In the IGE panel (top), each colour corresponds to a class of*
209 *phenotypes: behavioural (red, includes 7 behavioural phenotypes with a significant*
210 *IGE locus), adult neurogenesis (black, 2 phenotypes with a significant IGE locus),*
211 *immune (orange, 1 phenotype with a significant IGE locus), haematological (yellow, 1*
212 *phenotype with a significant IGE locus), blood biochemistry (blue, 2 phenotypes with*
213 *a significant IGE locus), bone phenotypes (green, 2 phenotypes with a significant IGE*
214 *locus), heart function (brown, 1 phenotype with a significant IGE locus), and lung*
215 *function (purple, 1 phenotype with a significant IGE locus). In the DGE panel (bottom),*
216 *the same colouring scheme is used as in the IGE panel except for grey dots, which*
217 *are for phenotypes that do not have any significant IGE locus.*

218 **Identification of putative causal genes for experimental evaluation**

219 Linkage disequilibrium decays faster in the CFW population than in many other mouse
220 populations used for mapping, which facilitates identification of putative causal genes
221 at associated loci(36, 37, 45). To identify such genes, we fine-mapped the 24
222 significant IGE loci using the full set of variants (rather than the pruned set used for
223 igeGWAS) in the 1.5Mb window surrounding the most significant variant at the locus,
224 which corresponds, in this sample, to the average 95% confidence interval for the
225 association(37). We then identified, for each significant IGE locus, all of the genes that
226 either overlapped the associated plateau or were located in direct proximity (see
227 Methods, genes listed in **Supplementary Table 3** and local association plots in
228 **locusZooms_SupplTable3.zip**). At seven loci there was a single putative causal
229 gene: *Abca12* at a locus for adult neurogenesis, *Epha4* (stress-coping strategy), *Pkn2*,
230 *Slit3* and *Pgk1-rs7* (at three different loci for sleep), *H60c* (home cage activity), and
231 *Adcy1* (osteopetrosis).

232 One example of a putative causal IGE gene identified via this strategy is *Epha4*, which
233 was identified at an IGE locus on chromosome 1 for immobility during the first two
234 minutes of the forced swim test (FST), a measure of stress-coping strategy(46)
235 (**Figure 4a** and **Supplementary Figure 5**). We focused on *Epha4* initially because it
236 was the only putative causal gene at a significant locus, the locus was in the top half
237 of the list in terms of significance, and a knockout mouse model was readily available
238 from a neighbouring institute.

239 *Epha4* encodes a synaptic protein that plays an important role in synaptic
240 plasticity in the hippocampus(47, 48) and DGE of *Epha4* on FST immobility have been
241 reported(49, 50). Therefore we evaluated the possibility that *Epha4* directly influences
242 stress-coping strategy and that the stress-coping strategy of a mouse in the weeks
243 prior to or during the FST gets copied by the other mice in the cage (behavioural
244 contagion), thereby giving rise to IGE on stress-coping strategy. To investigate this
245 hypothesis, we tested whether *Epha4* had direct effects on FST immobility in CFW
246 mice, using the full set of variants in the same 1.5Mb window including *Epha4* as for
247 IGE analysis. We found little evidence that *Epha4* directly affects FST immobility in
248 CFW mice (maximum -logP value at the locus: 2.14, **Figure 4b**), making it unlikely
249 that behavioural contagion explains the detected IGE in CFW mice.

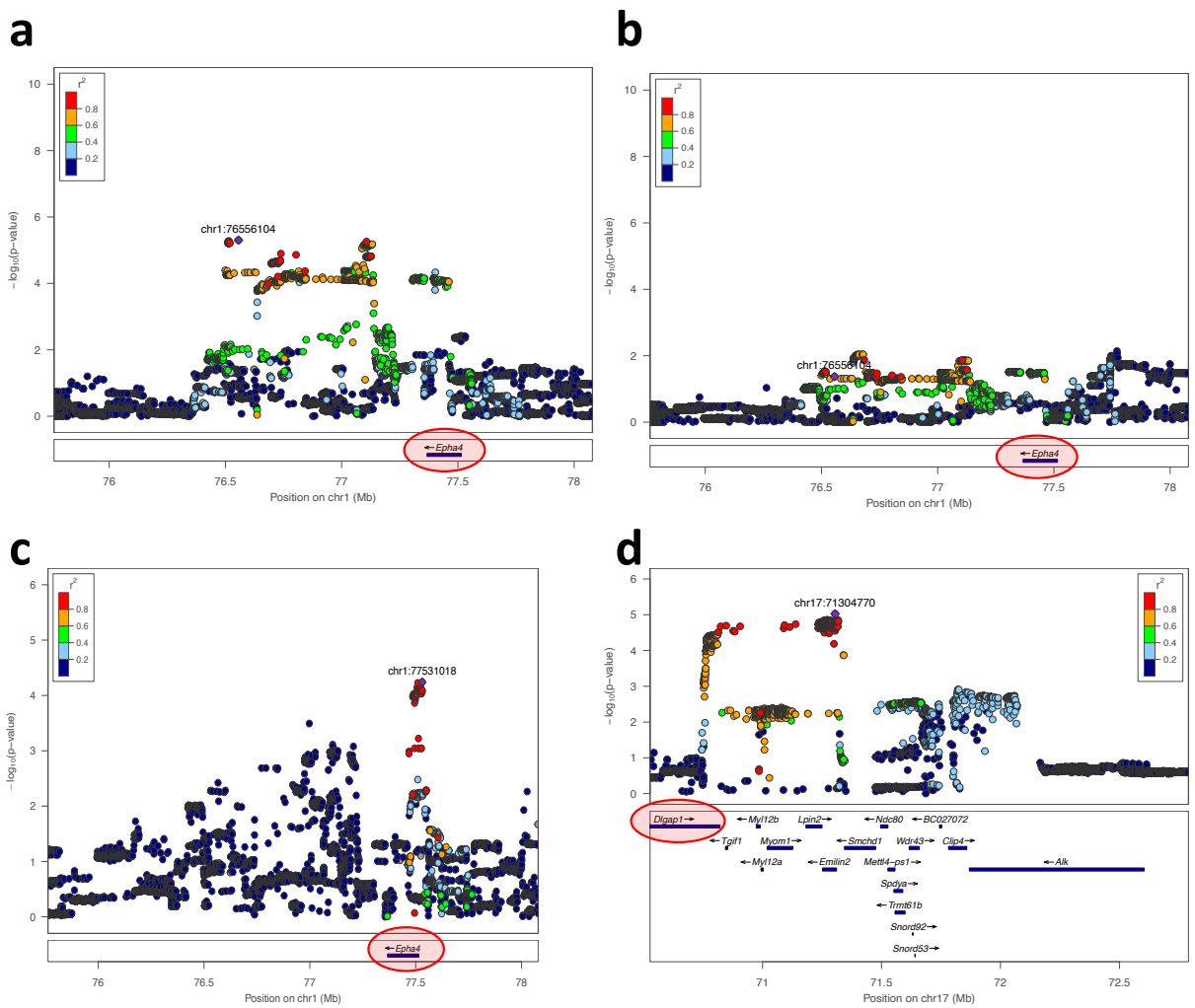

250

251 **Figure 4** *Locus zoom plots for the four associations in CFW outbred mice that were*
252 *subsequently tested in an experiment with Epha4 and Dlgap1 knockout models.* ***(a)***
253 *Significant IGE locus on chromosome 1 for immobility during the first two minutes of*
254 *the forced swim test (FST), a measure of stress-coping strategy. Epha4 was identified*
255 *as the only putative causal gene at this locus (see Methods).* ***(b)*** *Same locus and*
256 *phenotype but DGE, rather than IGE, are shown. The plot shows little evidence of*
257 *DGE on FST immobility at the Epha4 locus.* ***(c)*** *Suggestive IGE association at the*
258 *Epha4 locus with rate of healing from an ear punch, a phenotype of particular interest*
259 *(-logP = 4.1, FDR > 10%).* ***(d)*** *Second significant (FDR < 10%) IGE locus for immobility*
260 *in the FST (this time measured during the last four minutes of the test). Dlgap1 is one*

261 *of eight putative causal genes at this locus. It was singled out because of its functional*
262 *similarity and co-expression with Epha4 (see Text).*
263
264 In addition to the significant IGE association between *Epha4* and FST
265 immobility, we found suggestive evidence for an IGE association between *Epha4* and
266 rate of healing from an ear punch (igeGWAS -logP value = 4.1, FDR > 10%, **Figure**
267 **4c**). This finding was of particular interest because the *Epha4* locus was among the
268 three most significant IGE loci for wound healing (all three loci with -logP=4.1) and
269 because IGE on wound healing seem to be ubiquitous in laboratory mice: indeed, we
270 have found a significant *aggregate* contribution of IGE to rate of healing from an ear
271 punch in all three mouse populations we have looked at to date (inbred C57BL/6J mice
272 and outbred Heterogeneous Stock mice in Baud et al.(9), and CFW mice in this study).
273 Thus, we were particularly interested in testing whether *Epha4* was involved in IGE on
274 wound healing.
275 We found two additional significant IGE loci for FST immobility, more precisely
276 for immobility during the last four minutes of the test (**Supplementary Table 3,**
277 **Supplementary Figure 6a**). At the locus on chromosome 17, we identified eight
278 genes as putatively causal but singled out *Dlgap1* (**Figure 4d**) for experimental
279 validation because it encodes a synaptic protein(51), like *Epha4*, and because its
280 expression in the hippocampus, which was measured in a separate cohort of 79 male
281 CFW mice(45), was significantly and highly correlated with that of *Epha4* (Spearman
282 r = 0.868, Bonferroni-corrected P = $2{,}3.10^{-19}$, **Supplementary Figure 6b**). As was the
283 case for *Epha4*, we found no evidence of DGE arising from *Dlgap1* and affecting FST
284 immobility in CFW mice (maximum -logP value at the locus 2.46).

285 **Evaluating the role of *Epha4* and *Dlgap1* in IGE using knockout models**

286 We tested the hypotheses that *Epha4* can give rise to IGE on FST immobility and rate
287 of healing using a constitutive *Epha4* knockout model on a mixed C56BL/6 &
288 C56BL/10 genetic background. In addition, we tested for IGE from *Dlgap1* on FST
289 immobility using a constitutive *Dlgap1* knockout model on a C57BL/6N background.
290 At weaning, one *Epha4* mouse (heterozygote or wild-type, see Methods) or one
291 *Dlgap1* mouse (homozygote knockout, heterozygote or wild-type) was co-housed with
292 one focal FVB/NJ (FVB) mouse of the same sex (male or female). The FVB strain was
293 chosen because it is the *inbred* strain whose genetic background is most similar to
294 that of the *outbred* CFW mice used in igeGWAS, contributing 38% of all alleles in CFW
295 mice(37). Focal FVB mice were ear punched prior to pairing, then the pairs of mice
296 were left to interact in their cages for two months before they were all tested in the
297 FST and the ears of FVB mice were analysed to measure the rate of healing (see
298 Methods).

299 Although FVB mice are genetically similar to CFW mice, we observed that focal
300 FVB mice showed much less immobility during the first two minutes of the FST than
301 CFW mice (2.0 seconds on average across all FVB mice vs 12.2 seconds on average
302 across all CFW mice). Therefore, in our analysis of FVB focal mice we focused on
303 immobility during the last four minutes of the test, even though this measure showed
304 a lower association in igeGWAS than immobility during the first two minutes of the test
305 (-logP = 2.8 and 5.2 respectively).

306 When considering males and females together we found no effect of the
307 genotype of cage mates on either FST immobility (P = 0.52, ANOVA, N = 81) or wound
308 healing (P = 0.40, ANOVA, N = 85). However, model comparison using the Akaike
309 Information Criterion (AIC) suggested there was an interaction between sex and
310 genotype of the cage mate (i.e. IGE) for both FST immobility and wound healing, as

311 the model including an interaction term between sex and genotype of the cage mate
312 was favoured. Therefore, we considered the two sexes separately and observed, in
313 males but not in females, IGE on FST immobility (P = 0.054, ANOVA, N = 35) and
314 wound healing (P = 0.038, ANOVA, N = 38) (**Figure 5**). The detection of male-specific
315 IGE from *Epha4* on wound healing is consistent with the observation of stronger IGE
316 at the *Epha4* locus in male CFW mice compared to female CFW mice
317 (**Supplementary Figure 7a**). The detection of male-specific IGE on FST immobility,
318 on the other hand, was not expected from the analysis of CFW mice as similar effects
319 were observed in males and females (**Supplementary Figures 7b and 7c**). A
320 potential explanation for male-specific IGE on FST immobility in FVB focal mice is that
321 FVB females showed lower immobility than FVB males, hindering our ability to detect
322 genetic effects. Nevertheless, these experimental results support the hypothesis that
323 *Epha4* can give rise to IGE on FST immobility and wound healing in laboratory mice.
324 As was the case in CFW mice, we did not observe a direct effect of *Epha4* on
325 FST immobility whether all mice or males only were considered (P = 0.22 and 0.23
326 respectively, ANOVA, N = 81 and 35 respectively), indicating behavioural contagion is
327 unlikely to explain these IGE.
328 Finally, we found no evidence of IGE from *Dlgap1* on FST immobility.

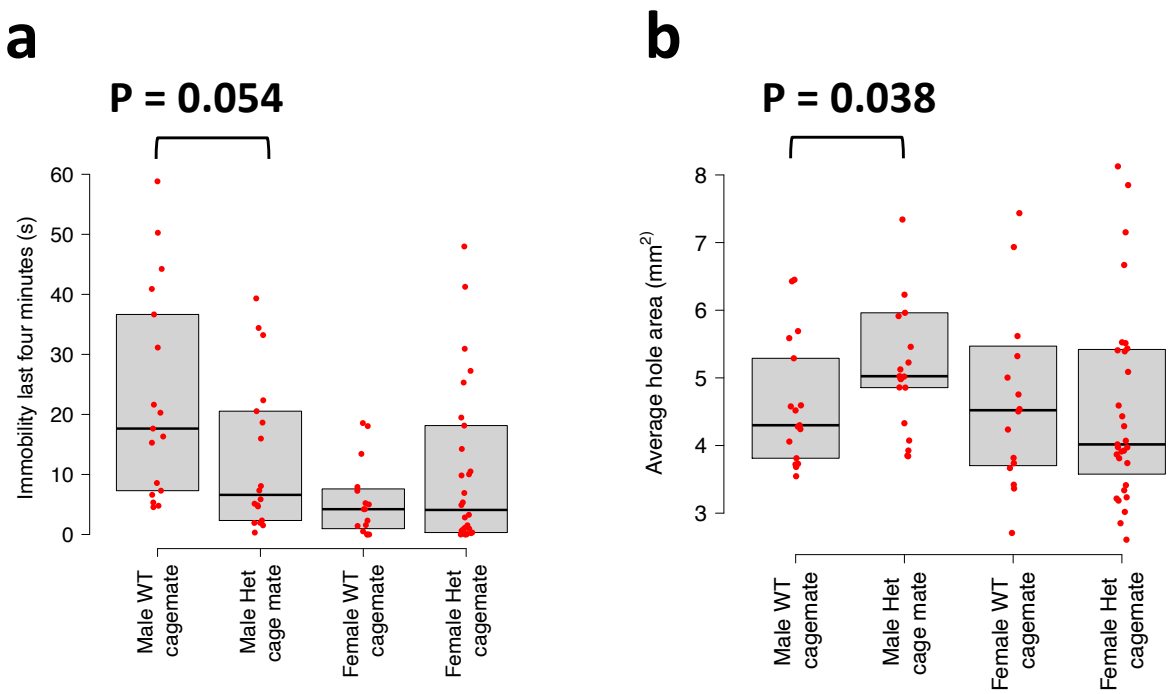

Figure 5 *Results of an experiment in which FVB focal mice were co-housed with Epha4 knockout heterozygote (Het) or wild-type (WT) cage mates. Immobility during the last four minutes of the FST* ***(a)*** *and rate of healing from an ear punch* ***(b)*** *were measured in FVB focal mice after two months of co-housing.*

Discussion

In this study, we leveraged a published dataset of 170 behavioural, physiological and morphological phenotypes measured in 1,812 genetically heterogeneous mice housed in same-sex groups of three to comprehensively assess the contribution of IGE to phenotypic variation and characterise the relationship between DGE and IGE for the same phenotype. Using polygenic models we showed that the genetic correlation ρ between DGE and IGE for a given phenotype is often significantly different from one, indicating IGE loci are different from DGE loci for the same phenotype. Consistently, we found that none of the 24 significant IGE loci identified for 17 phenotypes using igeGWAS overlapped with significant DGE loci identified using dgeGWAS. We fine-

345 mapped seven significant IGE loci to a single putative causal gene and experimentally
346 validated IGE from one of them, *Epha4*, on stress-coping strategy and wound healing
347 using a knockout model.

348 The analysis of the genetic correlation ρ between DGE and IGE for the same
349 phenotype provides insights into the overlap between DGE and IGE loci for a given
350 phenotype and whether the traits mediating IGE on a phenotype of interest are
351 genetically correlated (in the classical sense) with that phenotype. The correlation ρ
352 was expected to be different from zero for many phenotypes, based on reports that
353 emotions(52-54), behaviours(25, 55, 56), pathogens, and components of the gut
354 microbiome(57) can "spread" between individuals and contribute to phenotypic
355 variation, both in mice and in humans. In our study we found that ρ is significantly
356 different from zero for a variety of phenotypes, which indicates some overlap between
357 DGE loci and IGE loci for the same trait and is consistent with a genetic correlation (in
358 the classical sense) between the phenotype of interest and the traits mediating IGE.
359 However, we also found that ρ is significantly different from ±1 for ten out of twenty
360 eight traits, reflecting differences between DGE and IGE loci and demonstrating that
361 IGE on a phenotype of interest often involve traits of cage mates other than the
362 phenotype of interest. This was true even for phenotypes that likely spread, namely
363 stress and stress-coping strategies.

364 Consistent with the estimates of ρ from polygenic models, we found no overlap
365 between the 24 loci identified by igeGWAS for 17 phenotypes and the loci identified
366 by dgeGWAS for the same phenotypes. Our survey of a large number of phenotypes
367 suggests that the loci identified by igeGWAS will, generally, be different from those
368 identified by dgeGWAS, meaning igeGWAS holds great potential to uncover new loci

369 underlying phenotypic variation and that these loci will point to traits of cage mates
370 different from the phenotype studied.

371 Identifying IGE genes using igeGWAS has been previously attempted(5, 7, 8,
372 11, 31-35), but there has been limited evidence that this approach can indeed identify
373 genes that are causally involved in IGE. The results of our igeGWAS and fine-mapping
374 analyses identified a single putative causal gene at seven IGE loci: *Abca12* at a locus
375 for adult neurogenesis, *Epha4* at a locus for stress-coping strategy, *Pkn2*, *Slit3* and
376 Pgk1-rs7 at three different loci for sleep, *H60c* at a locus for home cage activity, and
377 *Adcy1* at a locus for osteopetrosis. We tested one of these genes, *Epha4*, as well as
378 another gene, *Dlgap1*, in experiments with knockout models. *Epha4* and *Dlgap1* were
379 putative causal genes at two different IGE loci for stress-coping strategy and both
380 encode synaptic proteins. However, only *Epha4* was at a locus with a single putative
381 causal gene, making it a stronger candidate than *Dlgap1*. We confirmed the role of
382 *Epha4* in giving rise to IGE on stress-coping strategy and wound healing in laboratory
383 mice, but did not find evidence of IGE from *Dlgap1*. A limitation of our experiment is
384 that FVB focal mice showed little to no immobility during the first two minutes of the
385 FST, in contrast with the CFW mice used in igeGWAS. Hence, even though the
386 significant igeGWAS locus was for immobility during the first two minutes of the test,
387 we had to focus on immobility during the last four minutes when analysing the
388 behaviour of FVB mice. Similarly, immobility during the last four minutes was lower in
389 FVB female mice than it was in FVB male mice, which may explain why only observed
390 IGE from *Epha4* in FVB male. Effects of the genetic background of knockout models
391 have been reported in studies of DGE(58); our results show that in studies of IGE both
392 the genetic background of the focal individuals matter too. In the future we will consider
393 a broader range of genetic backgrounds for focal mice. The seven genes listed above

394 as single putative causal genes at IGE loci as well as the experimental system we
395 have developed to test *Epha4* and *Dlgap1* will serve as valuable starting points to gain
396 further insights into the mechanisms of IGE in the future.

397 Finally, we identified challenges and solutions to different sources of
398 confounding in igeGWAS. In particular, we demonstrated that correlations between
399 direct and social genotypes arise when study individuals play both roles of focal
400 individuals and social partners and that, counter-intuitively, these correlations arise
401 even when all individuals are strictly unrelated. We showed that accounting for direct
402 effects of the locus tested in the null model for igeGWAS permits avoiding spurious
403 IGE associations. These insights, combined with the light we shed on two key
404 parameters determining the power of igeGWAS, namely the number of cage mates
405 and the mode of aggregation of IGE across cage mates, will inform the design and
406 analysis of future igeGWAS.

407

408 # Conclusions

409 Our results demonstrate the potential for igeGWAS to uncover genetic effects
410 expressed only in the context of social interactions and to serve as a starting point for
411 follow up analyses and experiments that will improve our understanding of peer effects
412 on health and disease.

413

414 # Methods

415 **Phenotypes and experimental variables**

416 Phenotypes and experimental variables (covariates) for 1,934 male and female
417 Crl:CFW(SW)-US_P08 (CFW) mice were retrieved from
418 http://wp.cs.ucl.ac.uk/outbredmice/. Phenotypes were normalized using the boxcox

419 function (MASS package(59)) in R; phenotypes that could not be normalised
420 satisfactorily (transformation parameter lambda outside of -2 to 2 interval) were
421 excluded. Because data for some phenotypes were missing for some mice, the sample
422 size varied. The sample size for each phenotype after all filtering (see below) is
423 indicated in **Supplementary Table 2**. The subset of covariates used for each
424 phenotype, which always included sex, is indicated in **Supplementary Table 2**. For
425 those phenotypes where body weight was included as a covariate, we checked that
426 this did not lead to systematically increased (or decreased) estimates of the aggregate
427 contribution of IGE (collider bias).
428
429 **Cage information**
430 Mice were four to seven weeks old when they arrived at the phenotyping facility and
431 were housed in same-sex groups of three mice. They were left undisturbed for nine to
432 twelve weeks during their time in quarantine and spent another four weeks together
433 during phenotyping.
434 Cage assignments were not included in the publicly available dataset but were
435 provided by the authors upon request and are now provided in **Supplementary Table**
436 **1**. Cage assignments were recorded at eleven time points throughout the study and
437 showed that a few mice were taken out of their original cages and singly housed,
438 presumably because they were too aggressive. We only included in our analyses mice
439 that had the same two cage mates throughout the experiment. We further excluded a
440 subset of mice based on their genotype-based genetic similarity, as described below.
441 Finally, all mice were singly housed during the sleep test and until sacrifice a few days
442 later. Hence, we investigated “persistent” IGE on sleep and tissue phenotypes.
443

444 **Genome-wide genotypes**

445 From http://wp.cs.ucl.ac.uk/outbredmice/ we retrieved both allele dosages for 7 million
446 variants and allele dosages for a subset of 353,697 high quality, LD-pruned variants
447 (as described in Nicod et al.(37); genotyping based on sparse sequencing data). We
448 used LD-pruned variants for all analyses but the identification of putative causal genes
449 at IGE loci (see below), for which we used the full set of variants.

450

451 **Genetic relatedness matrix (GRM) and exclusion of presumed siblings**

452 The genetic relatedness matrix was calculated as the cross-product of the LD-pruned
453 dosage matrix after standardizing the dosages for each variant to mean 0 and variance
454 1. A few pairs of mice were outliers in the distribution of GRM values, which made us
455 suspect that siblings had been included in the sample even though they were not
456 supposed to be (siblings were excluded by design). To mitigate confounding of DGE
457 and IGE analyses by litter effects, we excluded 19 cages (57 mice) from all analyses.

458

459 **Variance components model**

460 The same model as described in detail in Baud et al.(9) was used. Briefly, the model
461 used is the following:

462 $$y_f = X_f \underline{b} + a_{D,f} + e_{D,f} + Z_f \underline{a_S} + Z_f \underline{e_S} + W_f \underline{c} \qquad (0)$$

463 y_f is the phenotypic value of the focal mouse f, X_f is a row of the matrix X of covariate
464 values and b a column vector of corresponding estimated coefficients. $\underline{a_{D,f}}$ is the
465 additive direct genetic effects (DGE) of f. Z_f is a row of the matrix Z that indicates
466 cage mates (importantly $Z_{i,i} = 0$) and $\underline{a_S}$ the column vector of additive indirect (social)
467 genetic effects (IGE). $\underline{e_D}$ refers to direct environmental effects (DEE) and $\underline{e_S}$ to indirect

(social) environmental effects (IEE). W_f is a row of the matrix W that indicates cage assignment and c the column vector of cage effects.

The joint distribution of all random effects is defined as:

$$\begin{bmatrix} a_D \\ \hline a_S \\ \hline e_D \\ \hline e_S \\ \hline c \end{bmatrix} \sim \mathrm{MVN}\left(0, \begin{bmatrix} \sigma^2_{A_D}\mathrm{A} & \sigma_{A_{DS}}\mathrm{A} & 0 & 0 & 0 \\ \sigma_{A_{DS}}\mathrm{A}^T & \sigma^2_{A_S}\mathrm{A} & 0 & 0 & 0 \\ 0 & 0 & \sigma^2_{E_D}\mathrm{I} & \sigma_{E_{DS}}\mathrm{I} & 0 \\ 0 & 0 & \sigma_{E_{DS}}\mathrm{I}^T & \sigma^2_{E_S}\mathrm{I} & 0 \\ 0 & 0 & 0 & 0 & \sigma^2_C\mathrm{I} \end{bmatrix}\right)$$

where A is the GRM matrix and I the identity matrix.

The phenotypic covariance is:

$$\begin{aligned} C_{i,j} = cov\left(y_i, y_j\right) = {} & \sigma^2_{A_D} A_{i,j} + \sigma_{A_{DS}}\left\{(AZ^T)_{i,j} + (ZA^T)_{i,j}\right\} + \sigma^2_{A_S}(ZAZ^T)_{i,j} \\ & + \sigma^2_{E_D} I_{i,j} + \sigma_{E_{DS}}\left\{(IZ^T)_{i,j} + (ZI^T)_{i,j}\right\} + \sigma^2_{E_S}(ZIZ^T)_{i,j} \\ & + \sigma^2_C (WIW^T)_{i,j} \end{aligned}$$

When all cages have the same number of mice, as is the case in this study, the non-genetic random effects are not identifiable(15, 60). An equivalent model can, in that case, be defined as(60):

$cov\left(e_i, e_j\right) = \sigma^2_E = \sigma^2_{E_D} + 2\sigma^2_{E_S} + \sigma^2_C$ if $i = j$

$cov\left(e_i, e_j\right) = \rho_E\sigma^2_E = 2\,\sigma_{E_{DS}} + \sigma^2_{E_S} + \sigma^2_C$ if $i \neq j$ and i and j share a cage

$cov\left(e_i, e_j\right) = 0$ if i and j are in different cages

We checked that both model (0) and this alternative model yielded the same genetic estimates and maximum likelihoods. The alternative model was fitted using the SimplifNonIdableEnvs option in LIMIX(41, 61).

Aggregate contributions of DGE and IGE

The aggregate contributions of DGE and IGE were calculated, respectively, as $sampleVar\left(\sigma^2_{A_D} A\right) / sampleVar(C)$ and $sampleVar\left(\sigma^2_{A_S}(ZAZ^T)\right) / sampleVar(C)$, where $sampleVar$ is the sample variance of the corresponding covariance matrix: suppose that we have a vector $\underline{x}$ of random variables with covariance matrix M, the sample variance of M is calculated as

$$sampleVar(M) = \frac{Tr(PMP)}{n-1}$$

Tr denotes the trace, n is the sample size, and $P = I - \frac{11'}{n}$.

Significance of the IGE variance component was assessed using a two-degree of freedom log likelihood ratio (LLR) test (for the variance component and the covariance with DGE). Note that this testing procedure is conservative. The Q value for the aggregate contribution of IGE was calculated for each phenotype using the R package qvalue(62). Significant IGE contributions were reported at FDR < 10% (corresponding to Q value < 0.1).

Correlation between DGE and IGE

The correlation ρ between $\underline{a_D}$ and $\underline{a_S}$ was calculated as:

$$\rho = \frac{\sigma_{A_{DS}}}{\sigma_{A_D} \times \sigma_{A_S}}$$

We tested whether ρ was significantly different from 0 and whether |ρ| was significantly different from 1 using a one-degree of freedom LLR test, which is conservative for the latter test.

Simulations for Supplementary Figure 1.

Phenotypes were simulated based on the genotypes and cage relationships of the full set of 1,812 mice. Phenotypes were drawn from model (0) with the following

514 parameters: IGE explaining between 0 and 35.7% of phenotypic variance, DGE
515 explaining 15% of phenotypic variance, $\rho_{A_{DS}}$= 0.47, DEE explaining 22% of phenotypic
516 variance, IEE explaining 16% of phenotypic variance, $\rho_{E_{DS}}$ = -0.97, and cage effects
517 explaining 26% of phenotypic variance. These variances correspond to the median
518 value of estimates across traits with aggregate IGE and DGE > 5%. After building the
519 phenotypic covariance matrix, the sample variance of the simulations was calculated
520 and used to calculate "realised" simulation parameters from the "target" parameters
521 above. The realised parameters were used for comparison with the parameters
522 estimated from the simulations.
523

524 **Definition of "social genotype" for igeGWAS**

525 We assumed additive effects across cage mates and calculated the "social genotype"
526 of a mouse as the sum of the reference allele dosages of its cage mates. The same
527 assumption was made by Biscarini *et al.(40)* and Brinker *et al.(31)* among others.
528

529 **Models used for igeGWAS and dgeGWAS**

530 To test IGE of a particular variant in igeGWAS, we compared the following two models:

531 $y_f = X_f\underline{b} + a_{D,f} + e_{D,f} + Z_f\underline{a_S} + Z_f\underline{e_S} + W_f\underline{c} + G_f b_D$ (1, null)

532 $y_f = X_f\underline{b} + a_{D,f} + e_{D,f} + Z_f\underline{a_S} + Z_f\underline{e_S} + W_f\underline{c} + G_f b_D + Z_f G b_S$ (2, alternative)

533 Here, G is the vector of direct genotypes at the tested variant; hence, G_f is the
534 genotype of the individual that is phenotyped (*f*) and $Z_f G$ is the sum of the genotypes
535 of the two cage mates of *f*. b_D the estimated coefficient for local DGE and b_S the
536 estimated coefficient for local IGE. Note that Z_f could be defined as the average of the
537 genotypes of the two cage mates of *f*, in which case $\underline{b_S}$ would be doubled but the

538 igeGWAS P values would remain unchanged. In igeGWAS, we refer to the inclusion
539 of $G_f b_D$ in model (1, null) as "conditioning".
540 The models were fitted using LIMIX with the covariance of the model estimated
541 only once per phenotype, in the null model with no local genetic effect (model 0).
542 The significance of local IGE was calculated by comparing models (1) and (2)
543 with a 1-degree of freedom LLR test.
544 dgeGWAS was carried out by comparing model (2) above to the null model (3)
545 below:

546 $$y_f = X_f \underline{b} + a_{D,f} + e_{D,f} + Z_f \underline{a_S} + Z_f \underline{e_S} + W_f \underline{c} + Z_f G b_S \qquad \text{(3, null)}$$

547 In dgeGWAS, we refer to the inclusion of $Z_f G b_S$ in model (3, null) as "conditioning".
548

549 **Identification of significant associations**

550 We used a genome-wide permutation strategy to control the FDR for each phenotype,
551 as done by Nicod et al.(37). This strategy takes into account the specific patterns of
552 linkage disequilibrium present in the sample and identifies significant associations *for*
553 *each phenotype independently of the results for the other phenotypes in the dataset*.
554 More precisely, for each phenotype and for each type of genetic effect (direct and
555 indirect), we performed 100 "permuted GWAS" by permuting the rows of the matrix of
556 social (respectively direct) genotypes, and testing each variant at a time using the
557 permuted genotypes together with the un-permuted phenotypes, un-permuted
558 covariates, un-permuted GRM and un-permuted matrix of direct (respectively social)
559 genotypes (for conditioning)(41, 42). For a given P value x, the per-phenotype FDR
560 can be calculated as:

561 $$FDR(x) = \frac{\#\ loci\ with\ P < x\ in\ permuted\ data}{100\ \times\ \#\ loci\ with\ P < x\ in\ unpermuted\ data}$$

562 We reported those loci with FDR < 10%.

563

564 **Definition of putative causal genes at associated loci**

565 At each significantly associated locus we defined a 1.5Mb window centred on the lead
566 variant corresponding, in this sample, to the 95% confidence interval for the
567 association(37). We identified all the variants that segregate in this window based on
568 the full set of 7M variants and reran igeGWAS and dgeGWAS locally using all the
569 variants at the locus. We defined "putative causal genes" as those genes that either
570 overlapped the associated plateau or were located in direct proximity, and whose MGI
571 symbol does not start by 'Gm', 'Rik', 'Mir', 'Fam', or 'Tmem' in order to focus on genes
572 with known function and generate more tractable hypotheses on the pathways of
573 social effects.

574 We identified putative causal genes using locusZoom plots(63). To create them, we
575 used the standalone version of locusZoom
576 (https://genome.sph.umich.edu/wiki/LocusZoom_Standalone). The plots for all 24
577 significant IGE loci reported in Supplementary Table 3 are provided in
578 locusZooms_SupplTable3.zip.

579

580 **Gene expression in the hippocampus of an independent sample of CFW mice**

581 Gene expression in the hippocampus of an independent sample of 79 male CFW mice,
582 initially published in Parker et al.(45), was available from GeneNetwork
583 (http://gn2.genenetwork.org/)(64, 65). The data are accessible by selecting Mouse as
584 *Species*, CFW Outbred GWAS as *Group*, Hippocampus mRNA as *Type*, and UCSD
585 CFW Hippocampus (Jan17) RNA-Seq Log2 Z-score as *Dataset*. To retrieve the genes
586 whose expression is most highly correlated with that of *Epha4*, we entered "Epha4" in

587 the *Get Any* field. Following selection of the Epha4 record (click on
588 ENSMUSG00000026235), we used *Calculate Correlations* with Sample r as *Method*,
589 UCSD CFW Hippocampus (Jan17) RNA-Seq Log2 Z-score as *Database*, and
590 Spearman rank as correlation *Type*. **Supplementary Figure 6b** was obtained by
591 clicking on the value of the correlation between Epha4 and Dlgap1 expression levels
592 (column *Sample rho*).
593
594 **Variance explained by a significant association**
595 The variance explained by a significant IGE association was estimated in an extension
596 of model (0) with additional fixed effects for both direct and social effects of lead SNPs
597 at all significant IGE loci (the lead SNP being the SNP with the most significant P value
598 at the locus in the igeGWAS). After fitting the model, the variance was calculated as:

600 $$\frac{var(ZG\widehat{b_S})}{\sum var\left(X_c\widehat{b_c}\right) + \sum var\left(G\widehat{b_D}\right) + \sum var(ZG\widehat{b_S}) + sampleVar(C)}$$

599

601 where $sampleVar(C)$ is the sample variance of the covariance matrix in this model.
602 The variance explained by a significant DGE association was estimated in a
603 similar model but considering all significant DGE associations and
604 calculated as:

606 $$\frac{var(ZG\widehat{b_D})}{\sum var\left(X_c\widehat{b_c}\right) + \sum var\left(G\widehat{b_D}\right) + \sum var(ZG\widehat{b_S}) + sampleVar(C)}$$

605

607 **Simulations for Supplementary Figure 2b and 2c.**
608 Phenotypes were simulated based on the genotypes and cage relationships of the
609 1,812 mice. Null phenotypes (no local IGE) were simulated from model (1) as the sum
610 of random effects and local DGE. The following parameters were used for the random

611 effects: $\sigma^2_{A_D}$ = 20 and $\sigma^2_{A_S}$ = 20 (which correspond to high polygenic effects in the real
612 data), $\rho_{A_{DS}}$= 0.5, $\sigma^2_{E_D}$= 30, $\sigma^2_{E_S}$= 30, $\rho_{E_{DS}}$ = -0.97, σ^2_C = 25 (which are close to the median
613 of the corresponding estimates from the real data). Local DGE were simulated at
614 random variants in the genome to account for 20% of the phenotypic variance.
615
616 **Simulations for Supplementary Figure 4.**
617 Phenotypes were simulated based on the real genotypes but random cages.
618 Phenotypes were simulated as the sum of random and fixed effects using the following
619 models:
620 $y_f = X_f\underline{b} + a_{D,f} + e_{D,f} + Z_f\underline{a_S} + Z_f\underline{e_S} + W_f\underline{c} + G_f b_D$ for local DGE
621 $y_f = X_f\underline{b} + a_{D,f} + e_{D,f} + Z_f\underline{a_S} + Z_f\underline{e_S} + W_f\underline{c} + Z_f G b_S$ for local IGE
622 The following parameter values were used for the random effects: $\sigma^2_{A_D}$ = 17, $\sigma^2_{A_S}$ = 17,
623 $\rho_{A_{DS}}$= 0.65, $\sigma^2_{E_D}$= 19, $\sigma^2_{E_S}$= 15, $\rho_{E_{DS}}$ = -0.8, σ^2_C = 25. These values correspond to the
624 median estimates for phenotypes with aggregate IGE and DGE > 0.1.
625 Local DGE and IGE were simulated at variants with low MAF (MAF < 0.05), medium
626 MAF (0.225<MAF<0.275) or high MAF (MAF>0.45). Local IGE were simulated using
627 two alternative generative models: an "additive" model by using Z as in model (2) (i.e.
628 filled with 0s and 1s) or an "average" model by using $Z' = \frac{Z}{N}$, where $N = 2$. In all cases
629 (DGE, additive IGE and average IGE) we simullated an allelic effect of 0.2, which is
630 similar to the average allelic effect estimated in the igeGWAS. Power was calculated
631 at a genome-wide significance threshold of negative log P 5, which is similar to the
632 significance of associations detected at FDR < 10%.
633
634 **Experiment with *Epha4* and *Dlgap1* knockout mice**

635 *Experimental design*

636 All animal procedures were approved by the Institutional Animal Care and Use
637 Committee of the University of California San Diego (UCSD) and were conducted in
638 accordance with the NIH Guide for the Care and Use of Laboratory Animals. FVB/NJ
639 breeder mice were originally purchased from the Jackson Laboratory (Bar Harbor, MA,
640 USA), then bred on site. *Epha4* knockout mice (allele name: Epha4tm1Byd) on a
641 mixed C56BL/6 C56BL/10 genetic background, originally created by Dottori et al.(66),
642 were generously donated by Prof. Elena Pasquale (Sanford Burnham Prebys, San
643 Diego, CA, USA) then bred at UCSD. The mouse line C57BL/6N-
644 Dlgap1<em1(IMPC)Tcp> was made as part of the KOMP2-Phase2 project at The
645 Centre for Phenogenomics, Toronta, Canada. It was obtained from the Canadian
646 Mouse Mutant Repository and bred at UCSD. Breeding from heterozygous parents
647 produced, for *Dlgap1*, wild-type (WT), heterozygote (Het) and homozygote knockout
648 (KO) offspring. For *Epha4*, homozygote knockout offspring usually died before
649 weaning, leaving Het and WT offspring only. Within three days of weaning, we paired
650 one focal FVB mouse with either a *Dlgap1* (WT, Het or KO) or an *Epha4* (WT or Het)
651 cage mate of the same sex (male or female). Immediately prior to pairing, the FVB/NJ
652 mice were ear punched on each ear using 2-mm ear punch scissors. Pairs of mice
653 were then left to interact for two months before all mice were phenotyped in the forced
654 swim test (FST), sacrificed and the ears of FVB/NJ mice were collected. The sample
655 size was 52 *Epha4* Het mice and 33 *Epha4* WT mice for wound healing; for FST, there
656 were only 48 *Epha4* Het mice as one mouse died during the FST, two mice had to be
657 separated from their cage mate due to fighting in the days before the FST (but their
658 ears were still collected as this did not significantly change the healing time), and the
659 battery of the camera recording the FST ran out during the FST of the fourth mouse.

660 A small subset of mice were video recorded in a new enclosure for 24h a few days
661 before the FST but the data from this pilot project are not reported here. Throughout
662 the experiment all mice were housed on a 12h:12h light-dark cycle, with lights on at
663 06:00, and all behavioural testing occurred during the light phase of the light-dark
664 cycle.
665
666 *Forced swim test*
667 Following the same protocol as in the CFW study(37), mice were tested in the forced
668 swim test: they were placed for 6 minutes in 6'' wide x 12'' tall glass buckets filed with
669 water at 24-26°C. Mice were video recorded from the side and their immobility during
670 the first 2 and last 4 minutes of the test was scored by an observer blind to the
671 genotypes of the black (*Epha4* and *Dlgap1*) mice. The analysis of IGE focused on
672 immobility of FVB mice in the last four minutes of the test as FVB mice are rarely
673 immobile during the first two minutes of the test.
674
675 *Healing from an ear punch*
676 Both ears of FVB/NJ mice were punched with a 2mm-diameter ear punch scissor just
677 before the mice were paired with an *Epha4* or a *Dlgap1* cage mate at weaning.
678 Following the same protocol as in the CFW study(37), the ears were collected two
679 months later after sacrifice, stored in 10% buffered formalin phosphate until analysis.
680 To measure the area of the hole, each ear was mounted on an histology slide and
681 photos were taken from a fixed distance. Images were analysed with the ImageJ
682 software(67) and the average across the two ears calculated.
683
684 *Genotyping*

685 For genotyping *Epha4* mice, tail or ear biopsies were sent to Transnetyx Inc. for
686 genotyping (Transnetyx Genotyping Services, Cordova, TN). Transnetyx Inc. utilize
687 real-time PCR and duplicate sample processing to ensure the accuracy of each
688 mutation. Additionally, Sanger sequencing was performed to further validate the
689 results of the Transnetyx assays.
690 For genotyping *Dlgap1* mice, we used a multiplex PCR with primers:
691 *CCGTAAGTGAAGTCTCCATCAACAG (Fw1), CGGCTAGGATTTCAGAGTTTGTTC*
692 (Fw2) and *CTTCCTCTCCTACACCATCAACAC (Rev1)*, yielding a 308bp band in the
693 presence of a WT allele and a 392bp band in the presence of a knockout allele.
694
695 *Statistical analysis*
696 For both FST immobility and wound healing, five fixed-effect models were first
697 compared using AIC: a model with intercept only, a model with the sex of the pair
698 (focal animal and cage mate were always of the same sex), a model with the genotype
699 of the cage mate, a model with both sex and genotype of cage mate, and finally a
700 model with main effects of sex and genotype of cage mate and their interaction.
701 IGE were then tested in males only using an analysis of variance (ANOVA) with one
702 degree of freedom.
703

704 Declarations

705 *Ethics approval*
706 All animal procedures were approved by the Institutional Animal Care and Use
707 Committee of the University of California San Diego (UCSD) and were conducted in
708 accordance with the NIH Guide for the Care and Use of Laboratory Animals.
709

710 *Availability of data and materials*

711 Genotype and phenotype data from Nicod et al.(37) and Davies et al.(38) are available
712 from http://wp.cs.ucl.ac.uk/outbredmice/. Cage information is provided in
713 Supplementary Table 1.

714 All the scripts used in this study are available from http://github.com/limix/IGE.

715 LIMIX can be downloaded from http://github.com/limix/limix.

716

717 *Competing interests*

718 The authors declare that they have no competing interests

719

720 *Funding*

721 AB was supported by a fellowship from the Wellcome Trust (105941/Z/14/Z). This work
722 was partially supported by a pilot grant from NIH (P50DA037844 to AAP). The funders
723 had no role in the design of the study, analysis and interpretation of the results, nor in
724 writing the manuscript.

725

726 *Authors' contributions*

727 AB, AAP and OS designed the study. AB and FPC performed the analyses. JN
728 contributed the cage information. AB, ABL, NF, and CM performed the mouse
729 knockout experiments. All authors contributed to the interpretation of the data. AB,
730 FPC, AAP and OS wrote the manuscript.

731

732 *Acknowledgements*

733 The authors want to thank Drs. Na Cai, Robert W. Davies and Richard Mott for
734 facilitating access to the genotype data. The authors also thank Dr. Elena Pasquale

735 for generously providing mice from the *EphA4* knockout line, which was produced
736 thanks to funding from NIH grant NS087070.

737

738 # References

739 1. Griffing B. Selection in reference to biological groups I. Individual and group selection
740 applied to populations of unordered groups. Australian Journal of Biological Sciences.
741 1967;20(1):127-40.
742 2. Moore AJ, Brodie III ED, Wolf JB. Interacting phenotypes and the evolutionary
743 process: I. Direct and indirect genetic effects of social interactions. Evolution.
744 1997;51(5):1352-62.
745 3. Wolf JB, Brodie III ED, Cheverud JM, Moore AJ, Wade MJ. Evolutionary
746 consequences of indirect genetic effects. Trends in ecology & evolution. 1998;13(2):64-9.
747 4. Wolf JB, Mutic JJ, Kover PX. Functional genetics of intraspecific ecological
748 interactions in Arabidopsis thaliana. Philosophical Transactions of the Royal Society B:
749 Biological Sciences. 2011;366(1569):1358-67.
750 5. Bailey NW, Hoskins JL. Detecting cryptic indirect genetic effects. Evolution.
751 2014;68(7):1871-82.
752 6. Bleakley BH, Brodie ED. Indirect genetic effects influence antipredator behavior in
753 guppies: estimates of the coefficient of interaction psi and the inheritance of reciprocity.
754 Evolution. 2009;63(7):1796-806.
755 7. Ashbrook DG, Gini B, Hager R. Genetic variation in offspring indirectly influences the
756 quality of maternal behaviour in mice. Elife. 2015;4:11814.
757 8. Ashbrook DG, Sharmin N, Hager R, editors. Offspring genes indirectly influence
758 sibling and maternal behavioural strategies over resource share. Proc R Soc B; 2017: The Royal
759 Society.
760 9. Baud A, Mulligan MK, Casale FP, Ingels JF, Bohl CJ, Callebert J, et al. Genetic
761 variation in the social environment contributes to health and disease. PLoS genetics.
762 2017;13(1):e1006498.
763 10. Head ML, Berry LK, Royle NJ, Moore AJ. Paternal care: direct and indirect genetic
764 effects of fathers on offspring performance. Evolution. 2012;66(11):3570-81.
765 11. Mutic JJ, Wolf JB. Indirect genetic effects from ecological interactions in Arabidopsis
766 thaliana. Molecular ecology. 2007;16(11):2371-81.
767 12. Petfield D, Chenoweth SF, Rundle HD, Blows MW. Genetic variance in female
768 condition predicts indirect genetic variance in male sexual display traits. Proceedings of the
769 National Academy of Sciences. 2005;102(17):6045-50.
770 13. Wilson AJ, Gelin U, Perron M-C, Réale D. Indirect genetic effects and the evolution of
771 aggression in a vertebrate system. Proceedings of the Royal Society of London B: Biological
772 Sciences. 2009;276(1656):533-41.
773 14. Moore AJ, Haynes KF, Preziosi RF, Moore PJ. The evolution of interacting
774 phenotypes: genetics and evolution of social dominance. the american naturalist.
775 2002;160(S6):S186-S97.
776 15. Bergsma R, Kanis E, Knol EF, Bijma P. The contribution of social effects to heritable
777 variation in finishing traits of domestic pigs (Sus scrofa). Genetics. 2008;178(3):1559-70.

16. Ellen ED, Visscher J, van Arendonk JA, Bijma P. Survival of laying hens: genetic parameters for direct and associative effects in three purebred layer lines. Poultry science. 2008;87(2):233-9.
17. Alemu SW, Bijma P, Møller SH, Janss L, Berg P. Indirect genetic effects contribute substantially to heritable variation in aggression-related traits in group-housed mink (Neovison vison). Genetics Selection Evolution. 2014;46(1):30.
18. e Silva JC, Potts B, Gilmour A, Kerr R. Genetic-based interactions among tree neighbors: identification of the most influential neighbors, and estimation of correlations among direct and indirect genetic effects for leaf disease and growth in Eucalyptus globulus. Heredity. 2017;119(3):125.
19. Wilson A, Coltman D, Pemberton J, Overall A, Byrne K, Kruuk L. Maternal genetic effects set the potential for evolution in a free-living vertebrate population. Journal of evolutionary biology. 2005;18(2):405-14.
20. McAdam AG, Boutin S, Réale D, Berteaux D. Maternal effects and the potential for evolution in a natural population of animals. Evolution. 2002;56(4):846-51.
21. Hadfield JD, Burgess MD, Lord A, Phillimore AB, Clegg SM, Owens IP. Direct versus indirect sexual selection: genetic basis of colour, size and recruitment in a wild bird. Proceedings of the Royal Society B: Biological Sciences. 2006;273(1592):1347-53.
22. Kong A, Thorleifsson G, Frigge ML, Vilhjalmsson BJ, Young AI, Thorgeirsson TE, et al. The nature of nurture: Effects of parental genotypes. Science. 2018;359(6374):424-8.
23. Bates TC, Maher BS, Medland SE, McAloney K, Wright MJ, Hansell NK, et al. The Nature of Nurture: Using a Virtual-Parent Design to Test Parenting Effects on Children's Educational Attainment in Genotyped Families. Twin Research and Human Genetics. 2018:1-11.
24. Warrington NM, Beaumont RN, Horikoshi M, Day FR, Helgeland Ø, Laurin C, et al. Maternal and fetal genetic effects on birth weight and their relevance to cardio-metabolic risk factors. Nature genetics. 2019:1.
25. Sotoudeh R, Harris KM, Conley D. Effects of the peer metagenomic environment on smoking behavior. Proceedings of the National Academy of Sciences. 2019;116(33):16302-7.
26. Xia C, Canela-Xandri O, Rawlik K, Tenesa A. Evidence of horizontal indirect genetic effects in humans. Nature Human Behaviour. 2021;5(3):399-406.
27. Demange PA, Hottenga JJ, Abdellaoui A, Malanchini M, Domingue BW, de Zeeuw EL, et al. Parental influences on offspring education: indirect genetic effects of non-cognitive skills. biorxiv. 2020.
28. McGlothlin JW, Brodie III ED. HOW TO MEASURE INDIRECT GENETIC EFFECTS: THE CONGRUENCE OF TRAIT-BASED AND VARIANCE-PARTITIONING APPROACHES. Evolution. 2009;63(7):1785-95.
29. Bijma P. The quantitative genetics of indirect genetic effects: a selective review of modelling issues. Heredity. 2014;112(1):61.
30. Wilson AJ, Morrissey M, Adams M, Walling CA, Guinness FE, Pemberton JM, et al. Indirect genetics effects and evolutionary constraint: an analysis of social dominance in red deer, Cervus elaphus. Journal of evolutionary biology. 2011;24(4):772-83.
31. Brinker T, Bijma P, Vereijken A, Ellen ED. The genetic architecture of socially-affected traits: a GWAS for direct and indirect genetic effects on survival time in laying hens showing cannibalism. Genetics Selection Evolution. 2018;50(1):38.
32. Wu P, Wang K, Yang Q, Zhou J, Chen D, Liu Y, et al. Whole-genome re-sequencing association study for direct genetic effects and social genetic effects of six growth traits in Large White pigs. Scientific reports. 2019;9(1):1-12.

826 33. Hong J-K, Lee J-B, Ramayo-Caldas Y, Kim S-D, Cho E-S, Kim Y-S, et al. Single-step
827 genome-wide association study for social genetic effects and direct genetic effects on growth
828 in Landrace pigs. Scientific reports. 2020;10(1):1-11.
829 34. Warrington NM, Beaumont RN, Horikoshi M, Day FR, Helgeland Ø, Laurin C, et al.
830 Maternal and fetal genetic effects on birth weight and their relevance to cardio-metabolic risk
831 factors. Nature genetics. 2019;51(5):804-14.
832 35. McGinnis R, Steinthorsdottir V, Williams NO, Thorleifsson G, Shooter S, Hjartardottir
833 S, et al. Variants in the fetal genome near FLT1 are associated with risk of preeclampsia. Nature
834 genetics. 2017;49(8):1255.
835 36. Yalcin B, Nicod J, Bhomra A, Davidson S, Cleak J, Farinelli L, et al. Commercially
836 available outbred mice for genome-wide association studies. PLoS genetics.
837 2010;6(9):e1001085.
838 37. Nicod J, Davies RW, Cai N, Hassett C, Goodstadt L, Cosgrove C, et al. Genome-wide
839 association of multiple complex traits in outbred mice by ultra-low-coverage sequencing.
840 Nature genetics. 2016;48(8):912.
841 38. Davies RW, Flint J, Myers S, Mott R. Rapid genotype imputation from sequence
842 without reference panels. Nature genetics. 2016;48(8):965.
843 39. Sadler AM, Bailey SJ. Repeated daily restraint stress induces adaptive behavioural
844 changes in both adult and juvenile mice. Physiology & behavior. 2016;167:313-23.
845 40. Biscarini F, Bovenhuis H, Van Der Poel J, Rodenburg T, Jungerius A, Van Arendonk
846 J. Across-line SNP association study for direct and associative effects on feather damage in
847 laying hens. Behavior genetics. 2010;40(5):715-27.
848 41. Casale FP, Rakitsch B, Lippert C, Stegle O. Efficient set tests for the genetic analysis
849 of correlated traits. Nature methods. 2015;12(8):755.
850 42. Sudmant PH, Rausch T, Gardner EJ, Handsaker RE, Abyzov A, Huddleston J, et al. An
851 integrated map of structural variation in 2,504 human genomes. Nature. 2015;526(7571):75.
852 43. Beavis W. QTL analyses: power, precision and accuracy. Molecular Dissection of
853 Complex Traits. Edited by: AH P. 1997. CRC Press, New York.
854 44. Beavis W, Beavis W. The power and deceit of QTL experiments: lessons from
855 comparative QTL studies. 1994.
856 45. Parker CC, Gopalakrishnan S, Carbonetto P, Gonzales NM, Leung E, Park YJ, et al.
857 Genome-wide association study of behavioral, physiological and gene expression traits in
858 outbred CFW mice. Nature genetics. 2016;48(8):919.
859 46. Commons KG, Cholanians AB, Babb JA, Ehlinger DG. The Rodent Forced Swim Test
860 Measures Stress-Coping Strategy, Not Depression-like Behavior. ACS Chemical
861 Neuroscience. 2017;8(5):955-60.
862 47. Bouvier D, Corera AT, Tremblay MÈ, Riad M, Chagnon M, Murai KK, et al. Pre-
863 synaptic and post-synaptic localization of EphA4 and EphB2 in adult mouse forebrain. Journal
864 of neurochemistry. 2008;106(2):682-95.
865 48. Murai KK, Nguyen LN, Irie F, Yamaguchi Y, Pasquale EB. Control of hippocampal
866 dendritic spine morphology through ephrin-A3/EphA4 signaling. Nature neuroscience.
867 2003;6(2):153-60.
868 49. Li Y, Wang H, Wang X, Liu Z, Wan Q, Wang G. Differential expression of
869 hippocampal EphA4 and ephrinA3 in anhedonic-like behavior, stress resilience, and
870 antidepressant drug treatment after chronic unpredicted mild stress. Neuroscience letters.
871 2014;566:292-7.
872 50. Zhang J-c, Yao W, Qu Y, Nakamura M, Dong C, Yang C, et al. Increased EphA4-
873 ephexin1 signaling in the medial prefrontal cortex plays a role in depression-like phenotype.
874 Scientific Reports. 2017;7(1):7133.

51. Coba M, Ramaker M, Ho E, Thompson S, Komiyama N, Grant S, et al. Dlgap1 knockout mice exhibit alterations of the postsynaptic density and selective reductions in sociability. Scientific reports. 2018;8(1):1-12.
52. de Oliveira PC, Zaniboni CR, Carmona IM, Fonseca AR, Canto-de-Souza A. Preliminary behavioral assessment of cagemates living with conspecifics submitted to chronic restraint stress in mice. Neuroscience letters. 2017;657:204-10.
53. Bolger N, DeLongis A, Kessler RC, Wethington E. The contagion of stress across multiple roles. Journal of Marriage and the Family. 1989:175-83.
54. Haeffel GJ, Hames JL. Cognitive Vulnerability to Depression Can Be Contagious. Clinical Psychological Science. 2014;2(1):75-85.
55. Stickney JD, Morgan MM. Social housing promotes recovery of wheel running depressed by inflammatory pain and morphine withdrawal in male rats. Behavioural Brain Research. 2021;396:112912.
56. Clarke T-K, Adams MJ, Howard DM, Xia C, Davies G, Hayward C, et al. Genetic and shared couple environmental contributions to smoking and alcohol use in the UK population. Molecular psychiatry. 2019:1-11.
57. Ridaura VK, Faith JJ, Rey FE, Cheng J, Duncan AE, Kau AL, et al. Gut microbiota from twins discordant for obesity modulate metabolism in mice. Science. 2013;341(6150):1241214.
58. Sittig LJ, Carbonetto P, Engel KA, Krauss KS, Barrios-Camacho CM, Palmer AA. Genetic background limits generalizability of genotype-phenotype relationships. Neuron. 2016;91(6):1253-9.
59. Venerables W, Ripley B. Modern applied statistics with S. new york: Springer; 2002.
60. Bijma P, Muir WM, Ellen ED, Wolf JB, Van Arendonk JA. Multilevel selection 2: estimating the genetic parameters determining inheritance and response to selection. Genetics. 2007;175(1):289-99.
61. Lippert C, Casale F, Rakitsch B, Stegle O. LIMIX: genetic analysis of multiple traits. 2014.
62. Dabney A, Storey JD, Warnes G. qvalue: Q-value estimation for false discovery rate control. R package version. 2010;1(0).
63. Pruim RJ, Welch RP, Sanna S, Teslovich TM, Chines PS, Gliedt TP, et al. LocusZoom: regional visualization of genome-wide association scan results. Bioinformatics. 2010;26(18):2336-7.
64. Mulligan MK, Mozhui K, Prins P, Williams RW. GeneNetwork: a toolbox for systems genetics. Systems Genetics: Springer; 2017. p. 75-120.
65. Sloan Z, Arends D, Broman KW, Centeno A, Furlotte N, Nijveen H, et al. GeneNetwork: framework for web-based genetics. The Journal of Open Source Software. 2016;1(2):-.
66. Dottori M, Hartley L, Galea M, Paxinos G, Polizzotto M, Kilpatrick T, et al. EphA4 (Sek1) receptor tyrosine kinase is required for the development of the corticospinal tract. Proceedings of the National Academy of Sciences. 1998;95(22):13248-53.
67. Schneider CA, Rasband WS, Eliceiri KW. NIH Image to ImageJ: 25 years of image analysis. Nature methods. 2012;9(7):671-5.